Radiocarbon, Vol 60, Nr 5, 2018, p 1439–1455 DOI:10.1017/RDC.2018.115
Selected Papers from the 2nd Radiocarbon in the Environment Conference, Debrecen, Hungary, 3–7 July 2017

DEVELOPMENT OF SURFICIAL DEPOSITS ON BELYI ISLAND (KARA SEA) DURING THE LAST 40,000 YEARS

A Yurtaev[1*] • A Alexandrovskiy[2] • V Skripkin[3] • E Zazovskaya[2] • A Dolgikh[2,4]

[1]Tyumen State University, Institute of Environmental and Agricultural Biology (X-BIO), Tyumen, Russia.
[2]Institute of Geography, Russian Academy of Sciences, Department of Soil Geography & Evolution, Moscow, Russia.
[3]Institute of Environmental Geochemistry of NAS and MES of Ukraine, Kiev, Ukraine.
[4]The People's Friendship University of Russia (RUDN), Department of Science and Innovation Policy, Moscow, Russia.

ABSTRACT. A series of radiocarbon (^{14}C) dates of peat and other materials, containing organic matter, were obtained from Belyi Island. We have identified a large group of dates associates with MIS 1, as well as a significant group of dates associated with the Kargin (MIS 3) period (40–31 ka cal BP). A large number of dates from the Late Glacial period and from the Early Holocene (MIS 1—ca. 14–9 ka cal BP) point to this time interval being associated with warm climate conditions (the Holocene thermal maximum). The climate cooled off significantly during the Middle and Late Holocene, and the intensity of peat accumulation declined. The dates from the MIS 2 period are missing, due to the conditions of this period being extremely unfavorable for the accumulation of peat, as well as of other materials suitable for ^{14}C dating.

KEYWORDS: Arctic, buried peat, environment, Holocene, Late Pleistocene, marine transgression, paleoclimate, radiocarbon dating.

INTRODUCTION

The development of the environment of the Kara Sea (Figure 1) continental shelf islands during the final stages of the Pleistocene was characterized by significant changes, which transpired under the influence of fluctuations in climate and sea level. In this region, like in other regions of the Arctic, these processes were associated with the formation of complex sediments that include layers of peat and paleosols (Evseev and Svitoch 1979; Vasilchuk et al. 1983). What distinguished the climate of Siberia, compared to that of the European part of Russia, was an early advent of the thermal maximum in the beginning of the Holocene (Khotinski 1977)[1]. This is due to the fact that the influence of the Scandinavian ice sheet did not reach the north of Western Siberia. This fact makes the paleogeography of the Kara region similar to that of the Alaskan region. The latter area was not covered by a continental ice sheet either and the Holocene thermal maximum there fell between 11 and 9 ka BP, with the summer temperatures being 1.6 ± 0.8°C higher than in the present (20th century) (Kaufman et al. 2004).

Currently, there are very few studies of Holocene sediments in the Kara Sea region (Vasilchuk et al. 1983; Tarasov et al. 1995; Stein et al. 2004; Slagoda et al. 2013). It is worth noting the studies of paleo-peat sediments recovered from Sverdrup Island (Figure 1). According to radiocarbon (^{14}C) data from Sverdrup Island, the warming began during the Allerød interstadial, about 12,000 BP (14,000 cal BP) and stopped during the Holocene, around 9500 BP (10,500 cal BP). It is believed that such an early accumulation of peat, which continued throughout the Younger Dryas, was due to the specifics of climate in the coastal areas of the Arctic, i.e., warm Early Holocene was followed by a mid-Holocene cooling (Tarasov et al. 1995).

[1]According to Khotinski (1977), the thermal maximum in Siberia dates to the Boreal period 8300–8900 BP (cal 9300–10,050 BP). Thus, the thermal maximum in Siberia took place earlier than in the European part of Russia, but later than in the Siberian Arctic (and on the Arctic islands) (Tarasov 1995; our data).

*Corresponding author. Email: yurtaevgeo@yandex.ru.

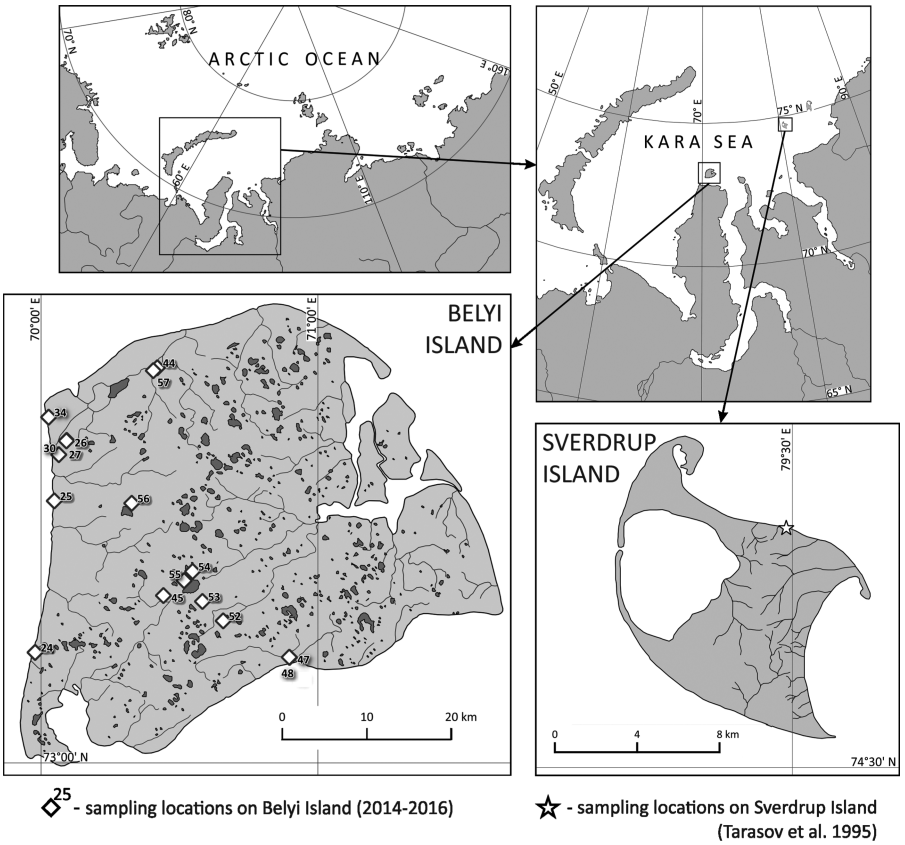

Figure 1 Map of Belyi and Sverdrup Islands (Kara Sea). Location of sites.

The above-mentioned trend is further confirmed by a northward spread of forests during the Early Holocene, which is confirmed by the ^{14}C dates of tree trunk fragments, found in the tundra (MacDonald et al. 2000). These climate changes resulted largely from fluctuations in sea level, which resulted in the exposure of significant areas of the continental sea shelf during cold spells of the Pleistocene (Tarasov et al. 1995; Vasil'chuk 2017a).

Fluctuations of sea level in Late Pleistocene-Holocene were associated with climate change. Cold climate of the last glacial maximum caused a deep regression of global sea level. Afterward, sea level started rising, but around 12,000 BP (cal 14,000 BP) it was still at a –70 to –80 m mark (Kaplin 1975; Kaplin and Selivanov 1999). At that time, the sea coast was 300–500 km north of its present position. During the Early Holocene 9000 BP (cal 10,000 BP), sea level rose to a –40 to –50 m mark and reached its current position only toward the middle of the Holocene (Stein et al. 2004; Gavrilov et al. 2006). After settling at its modern position, the sea began extending its cooling influence on modern coastal areas by causing a drop in the summer temperatures (Tarasov et al. 1995).

It is also worth mentioning that even during the period of thermal maximum, the climate of the territory in question remained cool. This in turn influenced the development of flora, as well as determined the character of soil formation processes (Gubin 1996; Kienast et al. 2005). Because until fairly recently there were very few ^{14}C dates from Belyi Island (Vasilchuk et al. 1983), we

https://doi.org/10.1017/RDC.2018.115 Published online by Cambridge University Press

could only hypothesize about the history and age of sediment formation there. The situation has changed only recently, after a significant number of ^{14}C dates were obtained from different parts of the island (Artemyeva et al. 2016; Alexandrovskiy et al. 2017; Baranskaya and Romanenko 2017; Baranskaya et al. 2018).

The purpose of our study was to reconstruct the history of sediment (and soil) formation on the island during Late Pleistocene and Holocene (last 40 ka BP), based on a series of ^{14}C dates of peat, as well as other carbon-containing materials.

MATERIALS AND METHODS

Peat and soil samples for ^{14}C dating were obtained from Belyi Island, which is situated north of Yamal Peninsula (73°15′00′′N, 70°50′00′′E) in the Kara Sea (Figure 1). While the island is of substantial size (50 × 40 km), it has low altitude (not exceeding 10 m asl). This fact is noteworthy because the development of the island during the Late Pleistocene and Holocene was associated with significant sea level fluctuations. The surface of the island can be classified as a low plain that was formed in the marine depositional environment. The transition from this plain to the island coast zone is rather abrupt and often has a shape of a ledge. The coastal zone incorporates beaches and low wet meadows. The altitude of the coastal areas does not exceed 1 m asl.

Sediments that form drainage divides mostly consist of sands that have different genesis. These sediments date to the Late Pleistocene (Slagoda et al. 2013). Throughout the island, there are many thermokarst lakes and round-shaped depressions. The river network mainly consists of small watercourses with poorly defined valleys that are often waterlogged. The watercourses flow in different directions and flow into the Kara Sea or its bays. Belyi Island is located within the Atlantic district of the Arctic climate belt. The climate of the island is characterized by especially long, harsh winters that are associated with severe storms and frequent blizzards. The warm period lasts only 55–70 days per year. The average yearly temperatures are negative—between –10°C and –12°C. Precipitation is low, less than 300 mm per year. However, the flat physical landscape and permafrost result in the island being covered with bogs (Abakumov et al. 2017).

Several types of geomorphic surfaces can be distinguished: marine terraces, their slopes, lacustrine depressions, riverine floodplains, and coastal marshes. Sedge-moss-cotton grass tundra communities predominate on elevated sites of marine terraces. In the depressions, they are replaced by sedge-sphagnum bogs. Dwarf shrub-sedge-lichen-moss communities have developed on drained slopes of the terraces. Forb-sedge and sedge-moss mires occupy waterlogged river valleys and lacustrine depressions. Low coastal marshes are covered by sedge-grass-moss communities. In general, forb-sedge-moss vegetation predominates on the island (Moskovchenko et al. 2017).

The soil cover patterns are controlled by the character of parent materials and topographic features. The major soil groups were determined in agreement with the legend to the Soil Map of the World (FAO-UNESCO 1997) and traditional Russian soil names. Tundra gley soils (Gelic Gleysols) occupy elevated terrace surfaces; in the depressions, they are replaced by peat gley soils (Gelic Histosols). Permafrost-affected podburs (Cryic Arenosols) have developed on slopes of the terraces composed of sandy material. Waterlogged depressions are occupied by hydromorphic permafrost-affected soils, which developed from alluvial, lacustrine, and marsh sediments (Fluvisols).

https://doi.org/10.1017/RDC.2018.115 Published online by Cambridge University Press

Morphological descriptions of soil and soil sampling were performed virtually across the entire territory of the island (Figure 1). In total, 16 pits were excavated, from which 40 samples of soil and organic matter were selected for ^{14}C dating (Table 1). Presently, all main parts of the island that are interesting from a paleogeographic perspective have been examined. Various sediment types have been sampled: mineral (marine clay loams, clays containing organic material, humified soil horizons) and organic (paleo-peat horizons, peat horizons of modern soils). A number of samples came from a marine terrace that was shaped by a mixture of abrasional and tectonic/depositional activities during the *Kargin interstadial* (MIS 3). The sediments associated with this terrace were located 2–4 m from the modern surface. They can be described as dark-gray and dark-green clay loam layers, which often included thin interlayers of detritus. These sediments were covered with sands of complicated genesis. In the upper portion, the sands often

Table 1 Brief descriptions of cross-section locations.

№	№ profile	Coordinates	Altitude (m asl)	Physical landscape zone	Notes
1	24	73°06′30″N 69°58′42″E	6	Sea shore	Southwestern part of the island
2	25	73°16′00″N 70°02′52″E	6	Sea shore	Northwestern part of the island
3	26	73°19′47″N 70°05′33″E	6	Drainage divide	Northwestern part of the island
4	27	73°19′45″N 70°05′30″E	5	Drainage divide slope	Northwestern part of the island
5	30	73°18′53″N 70°03′50″E	5	Drainage divide	Northwestern part of the island
6	34	73°21′13″N 70°01′38″E	4	Sea shore	Northwestern part of the island
7	44	73°24′17″N 70°25′11″E	7	Drainage divide	Northern part of the island
8	45	73°10′05″N 70°26′31″E	9	Drainage divide slope	Central part of the island
9	47	73°06′11″N 70°53′51″E	6	Sea shore	Southern part of the island
10	48	73°06′12″N 70°53′47″E	5	Drainage divide slope	Northern part of the island, close to cross-section №47, at the top of a gentle slope
11	52	73°08′29″N 70°39′28″E	5	Drainage divide	Central part of the island; the test pit was excavated in a small depression, associated with a dried out lake (50 m in diameter)
12	53	73°09′42″N 70°34′58″E	7	Drainage divide	Central part of the island
13	54	73°11′35″N 70°32′51″E	8	Lake shore	Central part of the island; in the vicinity of the Pahaayahanto Lake
14	55	73°11′01″N 70°31′00″E	4	Lake shore	Central part of the island; close to test pit №54; in the lower part of the lake shore
15	56	73°15′51″N 70°19′39″E	9	Lake shore	Western part of the island; in the vicinity of the Lyodseito lake
16	57	73°24′06″N 70°24′19″E	7	Drainage divide	Northern part of the island

https://doi.org/10.1017/RDC.2018.115 Published online by Cambridge University Press

had characteristics of redeposited sediments and included horizons and isolated pockets of buried peat. Most samples came from these redeposited materials. In addition, we took samples of in situ humified soil and peat horizons, which are often encountered on elevated drainage divides.

^{14}C age of the peat, total organic carbon (TOC) and humic acids from soils, lagoon, and lacustrine deposits, was determined by the liquid scintillation counting (LSC) method in the ^{14}C Laboratory of the Institute of Environmental Geochemistry of the National Academy of Sciences of Ukraine, Kiev (laboratory index Ki), in the Laboratory of Radiocarbon Dating and Electronic Microscopy of the Institute of Geography of the Russian Academy of Sciences in Moscow (IGAN).

Prior to the humic acids extracted, roots and plant debris were removed by sieving and flotation, carbonates were removed by repeated treatment with 1.0 M HCl until complete decalcination. Humic acids were repeatedly extracted with hot 0.1N NaOH. Humic acids were precipitated with H_2SO_4 in pH of 1–2, washed acid free and dried.

A sample containing peat is soaked in hot water for faster solubility of fulvic acids. Subsequently, peat fibers are separated from clay and sand through intensive shaking of the sampled material in sieves with proper mesh size. The filtered-out peat is submerged in a 2% hydrofluoric acid solution for 6 hr, while being periodically stirred. The remnants of carbonates and silicates are removed in the process. The humic acid particles, which got adsorbed to the surfaces of the mineral fraction, transition into a soluble state and dissolve during the subsequent washing. The peat, which remains on the surface of a fine-meshed sieve after washing, is dried at the temperature of 120–140°C. Finally, one obtains lithium carbide out of the resultant material through the vacuum pyrolysis technique (Skripkin and Kovalyukh 1998). The activity of ^{14}C was determined using a Quantulus 1220 liquid scintillation counter.

^{14}C dating of small samples was conducted in the Laboratory of Radiocarbon Dating and Electronic Microscopy of the Institute of Geography of the Russian Academy of Sciences (laboratory index $IGAN_{AMS}$). The dated marked $IGAN_{AMS}$ were obtained by accelerator mass spectrometry (AMS). The sample preparation for AMS (i.e., graphitization, pressing on a target) was performed in the Radiocarbon Laboratory of the Institute of Geography using the AGE-3 graphitization system (Ionplus). The dated fractions from the soil was the total organic carbon (TOC). The samples were cleaned of roots and plant debris in the laboratory. Then the samples were placed in 0.5M HCl and heated to 80ºC for 20 min to remove carbonates (Cheng et al. 2013; Zazovskaya et al. 2017), centrifuged, decanted, rinsed in deionized water and dried at 105ºC.

These samples were weighed into tin capsules and combusted in an elemental analyzer that transfers only the CO_2 in helium to the graphitization system. The elemental analyzer (EA) allowed fast combustion while maintaining a good separation of the combustion gases N_2 and H_2O from CO_2. Water was removed directly from the gas with a column filled with P_2O_5 (Sicapent™). The CO_2 is then trapped on zeolite while the helium carrier gas is removed. The CO_2 is thermally released and transferred to the reactors by gas expansion. The amount of CO_2 is kept constant to provide constant $CO_2/H_2/Fe$ ratios for the graphitization at 580°C (0.9 mg carbon, 4.2 mg iron, H_2/CO_2 ratio = 2.3). The water formed from the reduction is frozen in a Peltier cooled trap (about –5 °C). The reaction is stopped automatically after 2 hr when residual gas pressures are stable (for details see Wacker et al. 2010). The AGE 3 uses a Vario Micro Cube elemental analyzer from Elementar.

https://doi.org/10.1017/RDC.2018.115 Published online by Cambridge University Press

Graphite $^{14}C/^{13}C$ ratios were measured using the CAIS 0.5 MeV accelerator mass spectrometer in the Center for Applied Isotope Studies, University of Georgia (Cherkinsky et al. 2010). The sample ratios were compared to the ratio measured from the Oxalic Acid II (NBS SRM 4990C). The quoted uncalibrated dates have been given in ^{14}C years before 1950 (yr BP), using the ^{14}C half-life of 5568 yr. The error is quoted as one standard deviation and reflects both statistical and experimental errors. All of the ^{14}C dates were calibrated to calendar years using OxCal 4.3 software (Bronk Ramsey 2013) with use IntCal13 atmospheric curve (Reimer et al. 2013).

RESULTS

^{14}C dating of selected samples has indicated that the age of Quaternary sediments exposed in the coastal cross-sections approaches 40,000 years. It was impossible to excavate deep test pits because of the relatively high stratigraphic position of permafrost on the island. Therefore, deeper ancient horizons were examined in the cross-sections situated along the sea shore or along the banks of big island lakes.

We have identified three stratigraphic layers. At modern sea level, as well as the height of 1.5–2 m above it, in the southern and the southwestern parts of the island, we have identified dark-gray and grayish-green clay loams that date to the Kargin interstadial, 30–40 ka BP (Table 2). Above them are sands of complicated genesis, resulting from fluvial and marine sediments associated with MIS 3 being transferred into MIS 2 sediments. The resultant sand layers are 2 m and greater in thickness. The upper portions of these sand deposits were repeatedly affected by water erosion and accumulation processes. Sands that formed during MIS 1 and MIS 2 have often gotten redeposited; they often alternate with redeposited peat layers of Holocene and Late Pleistocene (Table 2 – profiles №25, 45, 47, 54).

Three main stratigraphic layers can be observed in cross-section 24. The upper layer, associated with MIS 1, is characterized by the presence of buried peat deposits, clay loam of alluvial/lacustrine(?) genesis, and modern Aeolian deposits. The middle layer, MIS 2, is associated with sand deposits. The lower, MIS 3, is associated with loam of lagoonal depositional genesis. The above layers were also identified in cross-sections 47, 54 and 55, 56. Deposits associated with MIS 1 and MIS 2 were identified in cross-section 25 (Figures 2a, 2b, 3).

Dates obtained via LSC and AMS methods coincided well with each other and followed the stratigraphic sequence of the sampled layers. This is well illustrated (Table 2; Figures 2a, 2b, 3) through layers associated with test pits №24 (24-1—AMS and 24-2—LSC), №47 (47-5—LSC and 47-6—AMS), №56 (56-2—LSC and 56-3—AMS). At the same time, chronological inversions can be observed in some occasions, e.g., in test pits №25 and 47 (Table 2, Figure 2a). These stratigraphic inconsistencies are not widespread; they formed due to the localized influences of water erosion in the past.

We distinguish two main groups of dates: 500–14,000 cal BP and 27,000–35,000 cal BP, associated with MIS 1 and MIS 3, corresponding to Holocene and the Kargin interstadial (Figure 4). Within MIS 1, the dates are distributed unevenly. There are few (only four) younger (<4500 yr) dates. There is a greater quantity (10) of dates belonging to the middle group (Middle and early Late Holocene). The greatest quantity of dates (21) is associated with the youngest Late Pleistocene–Early Holocene chronological group. The group of dates associated with the Kargin stage is non-numerous (6 dates); it is separated from the Holocene by MIS 2. The dates area missing for MIS 2 (Sartan cryochron). This is due to the fact that during MIS 2 the territory of Belyi Island was an icy desert, where the conditions did not allow

https://doi.org/10.1017/RDC.2018.115 Published online by Cambridge University Press

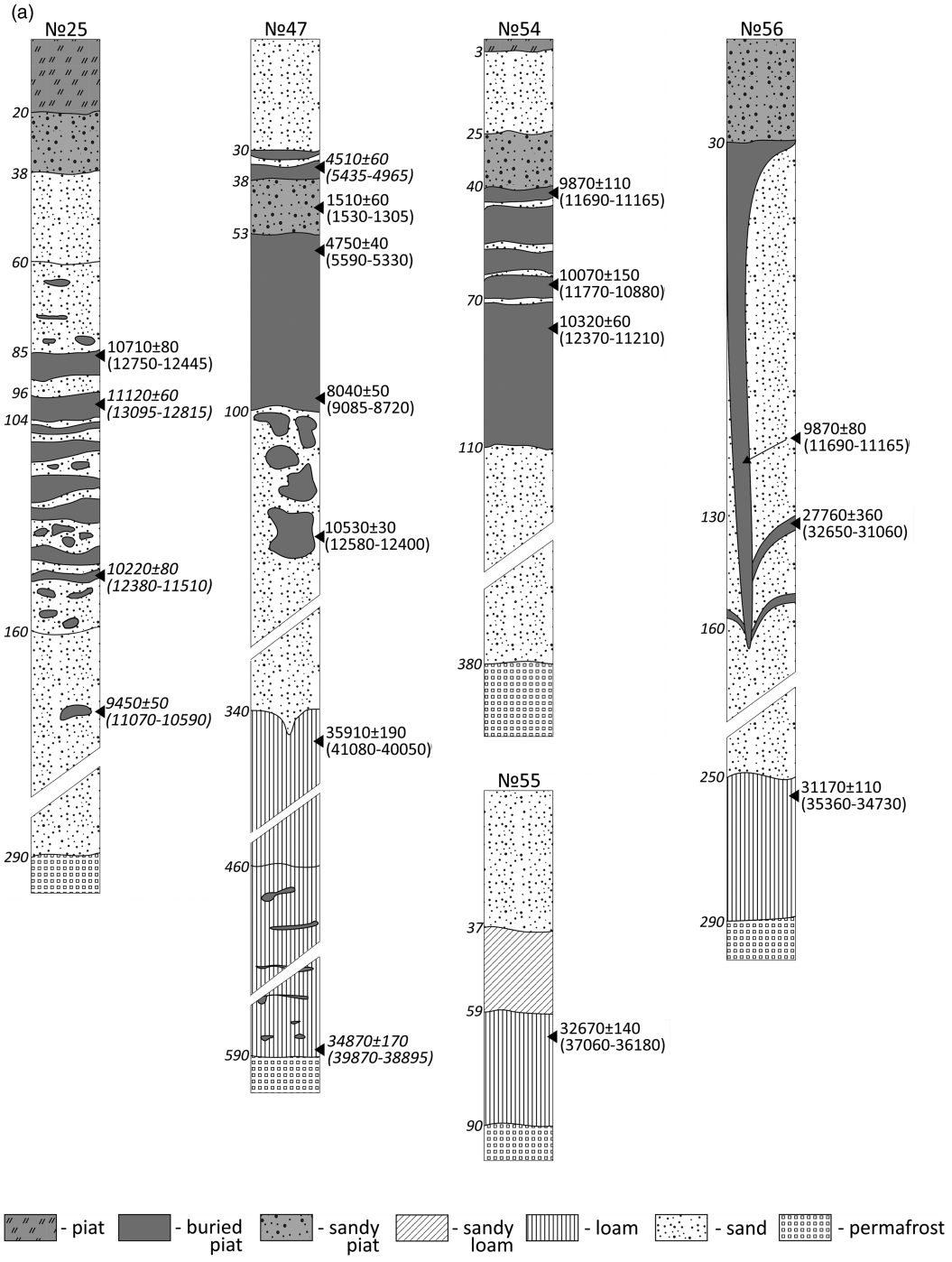

Figure 2 (a) Simplified stratigraphic profiles of pedo-sedimentological cross-sections of type 1, located along the seas and the lakes coast of Belyi Island. Cross-section numbers are provided above; depths levels in cm—on the left; radiocarbon dates (along with calibrated range)—on the right. Inversed dates from cross-sections 25 and 47 are italicized. Cross-section 25 contains peat layers with inversed chronology: a layer dating to 9450 ± 50 BP (10,708 ± 115 cal BP) had been redeposited first, while lower layers had been redeposited afterwards. In cross-section 47, the upper peat layers dating to 4510 ± 60 BP (5157 ± 104 cal BP) had been redeposited during the last 1500 years. This is evidenced by their position on top of a peat horizon that dates to 1510 ± 60 BP (1416 ± 65 cal BP). Deposits associated with MIS3 were also subject to redeposition—this is evidenced in the lower part of cross-section 47. (b) Simplified stratigraphic profiles of pedo-sedimentological cross-sections of type 1, located on the Island, away from the coast. Cross-section numbers are provided above; depths levels in cm—on the left; radiocarbon dates (along with calibrated range)—on the right.

https://doi.org/10.1017/RDC.2018.115 Published online by Cambridge University Press

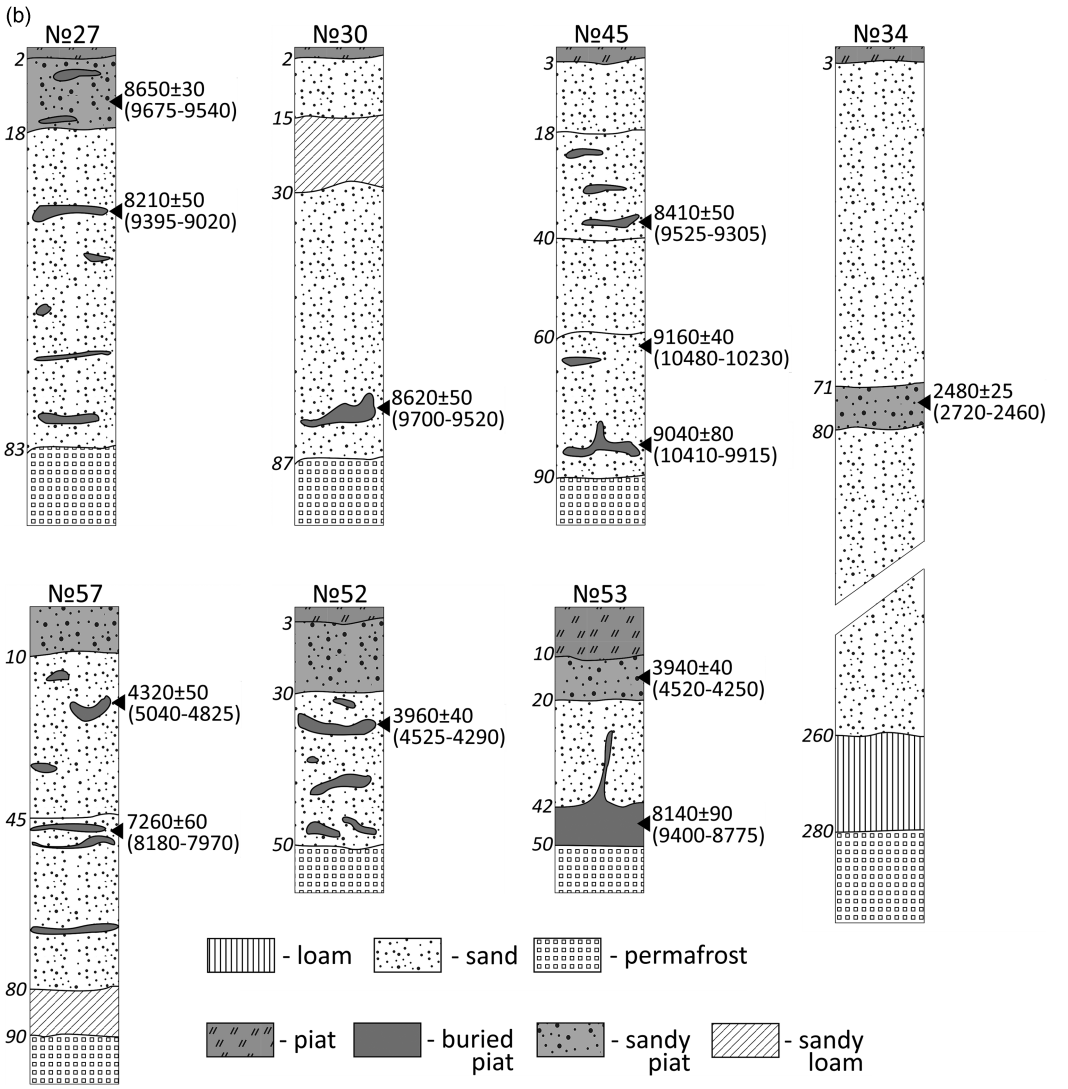

Figure 2 Continued.

the development of vegetation sufficient for the formation of organic deposits (Velichko et al. 2011).

We can distinguish a large number of dates from the Early Holocene and Late Glaciation, reaching into the Allerød interstadial. As already mentioned, this coincides with Khotinski's (1977) data that indicates an earlier onset of the thermal maximum (Early Holocene) in Siberia, compared to the European part of Russia. Our observations also coincide with Tarasov et al.'s (1995) data from the Sverdrup Island, where maximum temperatures are recorded for the 10,500–14,000 cal BP period.

The Kargin interstadial clay loam layers, which can be found under thick layers of sand all throughout the island, have a marine genesis. They are associated with the marine terrace of Belyi Island that was shaped by a mixture of abrasional and tectonic/depositional activities

https://doi.org/10.1017/RDC.2018.115 Published online by Cambridge University Press

(Slagoda et al. 2013). We have obtained samples from the western shore (sample 24-1—30,960–31,320 cal BP—Figure 3) and the southern shore (47-7—40,050–41,080 cal BP; 47-8—38,895–39,870 cal BP—Figure 2a). Two cross-sections containing these clay loam sediments were discovered in the central part of the island—near the Pahayahanto Lake (55-1—36,180–37,060 cal BP—Figure 2a) and on the Lyodseito Lake (56-3—34,730–35,360 cal BP—Figure 2a). In the southeastern part of the island, characterized by high (up to 6 m) shores with marine terrace coastline, the age of the Kargin terrace is also quite old—36–40 cal BP (Baranskaya and Romanenko 2017).

Thus, the age of Kargin clay loam sediments across the entire island's territory ranged from 40 to 31 ka cal BP (Table 2). It is noteworthy that the dates were the oldest in the southern and the southeastern parts of the island and younger in the western part of the island. It is necessary to mention that the position and character of Kargin clay loam sediments are complicated.

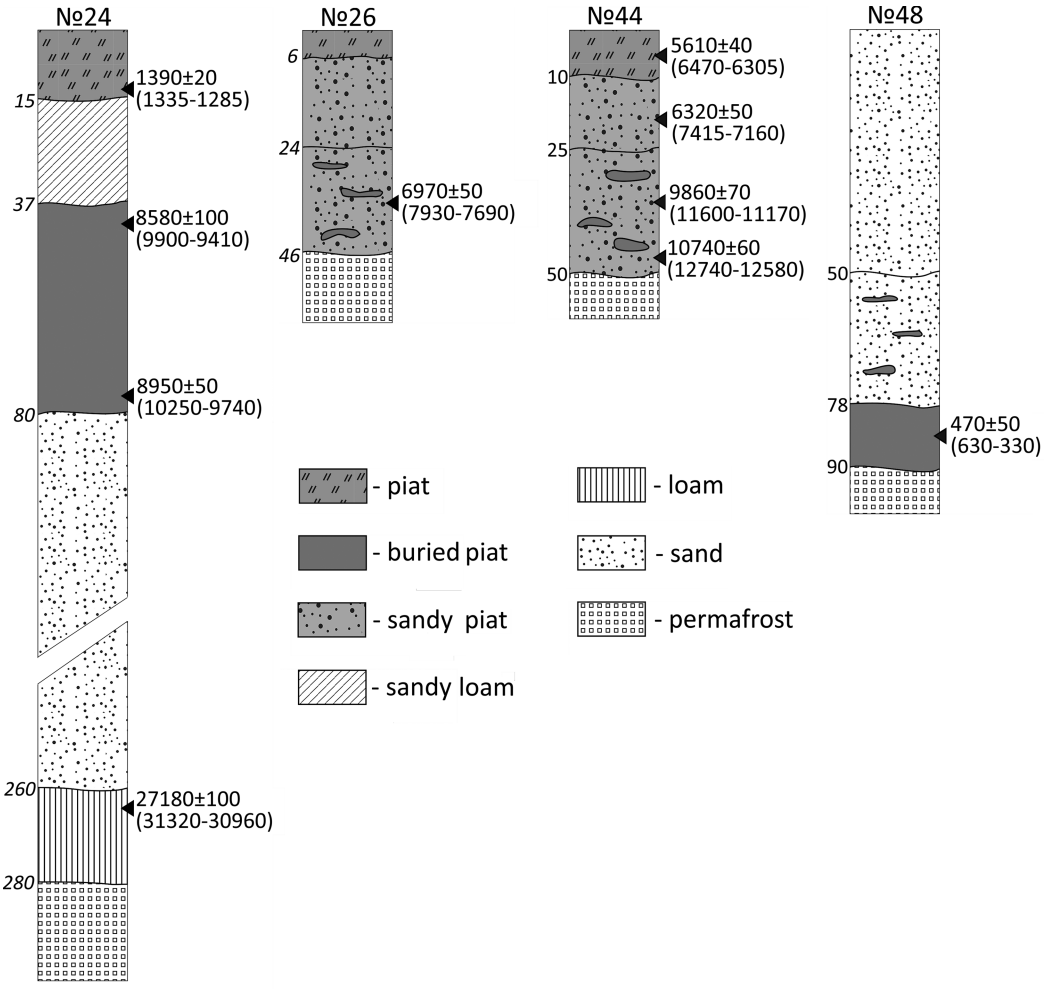

Figure 3 Simplified stratigraphic profiles of pedo-sedimentological cross-sections of types 2 (№24), 3 (№№ 26, 44) and 4 (№48) (Belyi Island). Cross-section numbers are provided above; depths levels in cm—on the left; radiocarbon dates (along with calibrated range)—on the right.

https://doi.org/10.1017/RDC.2018.115 Published online by Cambridge University Press

Table 2 Summary of ^{14}C dates from 40 organic matter samples taken from 16 cross-sections, placed in non-frozen loose surface deposits of Belyi Island. The dates were calibrated with the help of the OxCal 4.3 program (Bronk Ramsey 2013), using the IntCal13 calibration curve (Reimer et al. 2013).

Type of pedo-sediments[1]	№[2]	Sample description depth (cm)	Dated material	Lab code	Age		
					^{14}C yr BP	cal BP (2σ, 95.4 %)	Mean (μ) ± sigma (σ) cal BP
1st type: redeposited sand deposits with organic (paleo-peat) inclusions and horizons	25	25–1, 85–88	Peat	Ki 19230	10710 ± 80	12750–12445	12643 ± 61
		25–2, 96–104	Peat	Ki 19233	*11120 ± 60*[3]	*13095–12815*	*12972 ± 77*
		25–3, 145–150	Peat	Ki 19231	*10220 ± 80*	*12380–11510*	*11929 ± 178*
		25–4, 180–185	Peat	Ki 19223	*9450 ± 50*	*11070–10590*	*10708 ± 115*
	27	27–1, 10–13	TOC[4]	$IGAN_{AMS}$ 5395	8650 ± 30	9675–9540	9597 ± 39
		27–2, 37–40	Peat	Ki 19326	8210 ± 50	9395–9020	9175 ± 85
	30	30–1, 70–80	Peat	Ki 19220	8620 ± 50	9700–9520	9594 ± 52
	34	34–1, 71–80	Peat	Ki 19232	2480 ± 25	2720–2460	2585 ± 77
	45	45–1, 36–40	Peat	Ki 19325	8410 ± 50	9525–9305	9428 ± 59
		45–2, 60–65	Peat	Ki 19328	9160 ± 40	10480–10230	10324 ± 60
		45–3, 80–85	Peat	Ki 19323	9040 ± 80	10410–9915	10176 ± 127
	47	47–1, 30–38	Peat	Ki 19310	*4510 ± 60*	*5435–4965*	*5157 ± 104*
		47–2, 38–53	Peat	Ki 19324	1510 ± 60	1530–1305	1416 ± 65
		47–3, 53–60	Peat	Ki–19327	4750 ± 40	5590–5330	5486 ± 77
		47–4, 60–80	Peat	Ki–19333	7430 ± 60	8385–8065	8257 ± 66
		47–5, 80–100	Peat	Ki 19318	8040 ± 50	9085–8720	8903 ± 95
		47–6, 130–142	TOC	$IGAN_{AMS}$ 5396	10530 ± 30	12580–12400	12495 ± 51
		47–7, 340–360	TOC	$IGAN_{AMS}$ 5397	35910 ± 190	41080–40050	40557 ± 261
		47–8, 580–600	TOC	$IGAN_{AMS}$ 5398	*34870 ± 170*	*39870–38895*	*39386 ± 249*
	52	52–1, 30–40	Peat	Ki 19315	3960 ± 40	4525–4290	4420 ± 70
	53	53–1, 10–20	Peat	Ki 19316	3940 ± 40	4520–4250	4281 ± 70
		53–2, 42–50	Peat	Ki 19317	8140 ± 90	9400–8775	9096 ± ± 147
	54	54–1, 40–60	Peat	Ki 19334	9870 ± 110	11690–11165	11338 ± 128
		54–2, 60–70	Peat	Ki 19335	10070 ± 150	11770–10880	11370 ± 189
		54–3, 70–110	Peat	Ki 19336	10320 ± 60	12370–11210	11674 ± 267

	55	55–1, 59–90	TOC	$IGAN_{AMS}$ 5399	32670 ± 140	37060–36180	36591 ± 225
	56	56–1, 90–110	Peat	Ki 19319	9870 ± 80	11690–11165	11338 ± 128
		56–2, 130–142	Peat	Ki 19340	27760 ± 360	32650–31060	31738 ± 431
		56–3, 250–300	TOC	$IGAN_{AMS}$ 5400	31170 ± 110	35360–34730	35037 ± 158
	57	57–1, 24–33	Peat	Ki 19337	4320 ± 50	5040–4825	4909 ± 65
		57–2, 45–50	Peat	Ki 19339	7260 ± 60	8180–7970	8082 ± 62
2nd type: in situ paleo peat soils and pedosediments	24	24–1, 13–15[5]	Peat	$IGAN_{AMS}$5329/ UG_{AMS} 27737	1390 ± 20	1335–1285	1304 ± 12
		24–2, 40–50	HA[6]	IGAN 5009	8580 ± 100	9900–9410	9601 ± 125
		24–3, 70–80	HA	IGAN 5010	8950 ± 90	10250–9740	10036 ± 138
		24–4, 260–268	TOC	$IGAN_{AMS}$5330/ UG_{AMS} 277383	27180 ± 100	31320–30960	31139 ± 89
3rd type:in situ eroded peat soils	26	26–1, 30–40	Peat	Ki 19321	6970 ± 50	7930–7690	7804 ± 63
	44	44–1, 0–10	Peat	Ki 19329	5610 ± 40	6470–6305	6382 ± 45
		44–2, 10–25	Peat	Ki 19330	6320 ± 50	7415–7160	7250 ± 63
		44–3, 32–38	Peat	Ki 19331	9860 ± 70	11600–11170	11307 ± 104
		44–4, 45–50	Peat	Ki 19332	10740 ± 60	12740–12580	12672 ± 41
4th type[7]	48	48–1, 78–90	Peat	Ki 19320	470 ± 50	630–330	507 ± 52

[1]Detailed description in the text.[2]Numbers that were assigned to cross-sections during field research.[3]Dates with reversed chronology.[4]Total organic carbon.[5]The horizon 24-1, 13–15 cm refers to the 4th type.[6]Humic acids.[7]Modern aeolian-cumulative peat-sandy stratified soils.

Usually, they are represented by lagoonal clay loam deposits, which may include detritus, allochthonous peat, particles of wood, isolated pockets and even larger formations of moss. The age of these deposits coincides with the second half of MIS 3—37–40 ka cal BP (Baranskaya and Romanenko 2017).

We have also noted an inversion of dates in cross-section 47 (southern shore). Samples 47-7 and 47-8 were obtained from the depths of 3.4–3.6 and 5.8–6.0 m, respectively (Figure 2a). The upper horizon was more than 1000 yr older than the younger horizon, which may indicate redeposition of old sediments. Considering this inversion, as well as other morphological characteristics, we can conclude that the surface of the Kargin clay loam terrace underwent erosion and accumulation processes (these processes are usually associated with date inversions).

Above the Kargin clay loam layers, there is a thick accumulation of sand deposits that have a complicated genesis. The thickness of sand ranges from two to five meters. The sand sediments can be discerned into two components: the lower in situ and the upper redeposited ones. The lower part of the sand sediment typically has no organic inclusions. Therefore, ^{14}C dating of these sands is problematic. At the same time, in cross-section 56 (Lake Lyodseito), in the lower part of the sand profile, we have encountered sub-horizontal interlayers of detritus (56-2). Their age was 31,060–32,650 cal BP. This finding allows to associate the beginning of the sand layer accumulation to the end of the Kargin interstadial (MIS 3).

The upper layers of the sand deposit contain the most pedosediments. This fact can be attributed to the relatively recent age of these deposits, as well as to the intensity of the transformations that they underwent during the Holocene. Out of the materials recovered during our study, four types of pedosediments can be distinguished.

The first type—redeposited sand deposits with organic (paleo-peat) inclusions and horizons. These are encountered across the entire island at different altitudes (3–10 m asl) in all major geomorphological levels. The age of the paleo-peat in these deposits varies widely, from 13,000 to 1500 cal BP. At the same time, dates that fall into the Allerød interstadial and the Early Holocene prevail: cross-sections 25, 27, 30, 45, 47, 53, 54, 56 (Figure 2a).

In some cross-sections, the paleo-peat in the lower part of the profile produced early dates, while the upper part contained peat that formed in the Middle and Late Holocene. Such cross-sections were encountered in almost all parts of the island: cross-sections 34, 47, 52, 53 (Figure 2b).

Some cross-sections described above (25 and 47) were associated with date inversions. While in cross-section 25 (northwestern part of the island) the inversion concerns Early Holocene dates, the inversion associated with cross-section 47 concerns Late Holocene. Additionally, an inversion associated with the late Kargin period (MIS 3) was identified in the lower part of cross-section 47. Water erosion is the probable cause of the inversions in profiles 25 and 47. This conclusion is based on the morphological features of these deposits: wavy sub-horizontal borders; the presence of thin sand lenses in the peat and vice versa (presence of peat lenses in the sand layers).

The second type includes in situ paleo-peat soils and pedosediments that date to the Early Holocene. Such pedosediment was encountered on the southwestern shore of the island, in cross-section 24 (Figure 3). It had a typical stratigraphy: (1) starting at 2.6 m from the bottom

https://doi.org/10.1017/RDC.2018.115 Published online by Cambridge University Press

we see marine clay loam of the late Kargin time (24-4); (2) these deposits are covered by sands with complicated genesis; (3) at the depth of 220 cm from the sea level (80 cm from the surface) begins a peat horizon that is more than 40 cm thick. The age of the latter layer changes from 10,000 to 9600 cal BP, from the bottom up. (4) Above, the peat is cryoturbated clay loam deposits that are more than 20 cm thick. (5) Above these deposits lay modern aeolian-cumulative peat-sandy stratified soils that date to the Late Holocene.

The third type is in situ eroded peat soils. Such deposits were identified in the northern part of the island—cross-sections 26 and 44 (Figure 3). Cross-section 44 is the most illustrative in this regard. Here, in a disturbed peat layer that is 40 cm thick, the dates range from Early Holocene (44-4) to Middle Holocene cal BP (44-1), going from the bottom up. That way, mid-Holocene peat is observed at the surface (0–10 cm).

The fourth type includes modern aeolian-cumulative peat-sandy stratified soils (younger than 1500 cal BP). Such pedosediments form in the coastal zones—cross-section 48 (Figure 3). They date to the Late Holocene, starting from 1500 BP cal BP. A pseudomorph, identified in cross-section 56 (Figure 2) deserves particular attention. Filled with Early Holocene Peat, it crosses sand deposits and peat deposits of the final part of MIS 3 (3,1060–32,650 cal BP). The melting of the ice that filled the cracks took place in the beginning of MIS 1. The pseudomoprh was filled with peat which had formed by then (the dates of the peat are 11,165–11,690 cal BP (Table 2). The formation of the ice-filled crack could have only happened during MIS 2, when the winter temperatures were low enough for the formation of cryogenic cracks in the sand deposits. The Early Holocene–Late Pleistocene periods provided no such conditions: the north of Western Siberia witnessed a 4–5°C rise in the winter temperatures during the MIS 2–MIS 1 transition (Streletskaya et al. 2015).

DISCUSSION

Our data confirm the notion that Siberia experienced thermal maximum earlier that the European part of the country (Table 3). This conclusion is based on the faster rates of peat accumulation during the Allerød and the Younger Dryas periods, compared to the Middle Holocene on the Belyi Island and on other islands in the Kara Sea. On Belyi Island, the palynological spectra of paleo-peats dating to the beginning of MIS 1 is dominated arboreal pollen (mainly birch). This fact indicates that trees grew on the territory that is presently taken up by tundra. (Vasil'chuk 2017b). Arctic plants began dominating in the Middle and Late Holocene. Analogous vegetation changes have been recorded on the Sverdrup Island (Tarasov et al. 1995). The warming during the beginning of MIS 1 as well as the cooling of the Middle Holocene in the north of Western Siberia and in the Kara Sea region are attributed to a transgression. The MIS 2 cooling, which caused a drop in sea level by 120 m, exposed large areas of the arctic ocean (Stein et al. 2004.). The Kara sea shore receded by 300 km. The warming of the end of MIS 2–beginning of MIS 1 caused the degradation of the Scandinavian and other ice sheets and led to the transgression of the world ocean (Velichko et al. 2017). The rise in the sea level transpired gradually; it was still low during MIS 1 (more than 60 m) and the sea shore was far to the north (>200 km) of its present location. Due to these factors, the territory of the Belyi Island was inland, and, therefore, isolated from the cooling influence of the ocean during the summer. Only by 8000 cal BP the sea approached and surrounded the island. Meanwhile, the summer temperatures dropped by more than 1.5–2°C (Kaufman et al. 2004). This trend was especially well-pronounced on Sverdrup Island, where the accumulation of peat began earlier than on Belyi Island (13.8 ka cal BP), and continued during the Younger Dryas (Tarasov et al. 1995).

https://doi.org/10.1017/RDC.2018.115 Published online by Cambridge University Press

Table 3 Developmental stages of the environment and sediments of Belyi Island during the last 40 ka BP (the table summarizes our primary data).

MIS	Period	^{14}C age (cal BP)	Developments
3	Kargin thermochron	> 28000	Climate warming, sea level close to present, peats formed and got buried under the aeoloan sands.
2	Sartan cryochron, LGM	28000–14000	Deep sea regression (up to –120 m), reduction of the Arctic Ocean's area, formation of aeolian sands.
1	Allerød–Early Holocene	14000–9000	Sea level at –80 to –20 m, thermal maximum, active formation and burial of peat as a result of various processes.
	Middle and Late Holocene	9000–3500	Climate cooling; high sea level, at times higher than in the present; localized peat burial processes.
	Present period	<3500	Further cooling; aeolian accumulation in the coastal zone during the last 1500 yr.

The climate during the Late Glacial period–Early Holocene stage was relatively stable, as evidenced by a large quantity of peat formation dates from the 13–9 ka cal BP interval. The Allerød period on Belyi Island is associated with only one date, while on the nearby Sverdrup Island (also located in the Kara Sea; maximum altitude of 33 m asl) peat has formed all throughout the Allerød period. The buried peat deposit was discovered in the northwestern part of the island (Figure 1) at the altitude of 7–8 m asl within 6 m from the shore line (Tarasov et al. 1995). Therefore, it seems that the accumulation of peat transpired not only during the Allerød, but during the Younger Dryas as well. Palynological data (Tarasov et al. 1995) points to a cooling in the Younger Dryas. However, during that time shrub tundra prevails and the peat keeps accumulating (similar to Belyi Island). The Middle and Late Holocene cooling appears to have been more significant, compared to the Younger Dryas period. This trend is confirmed by palynological data from Sverdrup Island, as well as by a significant reduction of peat accumulation rates in the Kara Sea basin. Similar trends in climate and in the environmental development are characteristic of other Arctic regions (Gavrilov et al. 2006).

During the transition to the Middle Holocene, the character of sediment deposition has changed, as evidenced by the sediments of the first, second, and third types, described above. Sand deposits of the first type are widely distributed across the entire island's territory. The development of these deposits can be linked to sea transgressions, the height of which in the eastern regions of the Arctic has reached and exceeded 7 m asl (Bolshiyanov et al. 2015). In the area of our study, traces of such a transgression were not found. We think such processes started around 7–8 ka BP because before then, the sea level was tens of meters below its modern mark. Only Middle and Late Holocene peat layers can be considered buried under marine deposits. Additionally, the development of sand deposits on the island can be attributed to aeolian processes, which could transpire above the marine transgression mark during the last 8 ka. Before this time period, both aeolian and fluvial processes transpired across the entire territory of the island.

It is during this time that the conditions of peat accumulation (third type) have changed. The favorable conditions of Early Holocene have transitioned to the cooler Middle Holocene and (especially) Late Holocene periods. Mid-Holocene was associated with another factor that has influenced the evolution of organic layers—the marine transgression and the associated erosion

https://doi.org/10.1017/RDC.2018.115 Published online by Cambridge University Press

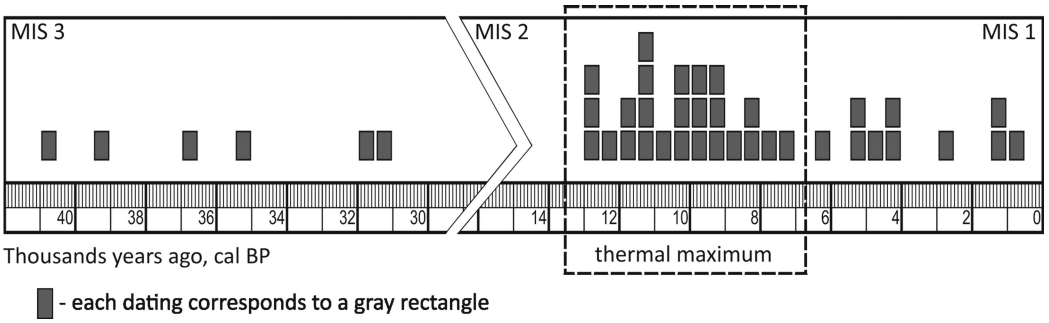

Figure 4 Distribution of radiocarbon dates along a time scale.

caused by sea water. As a result, the mid-Holocene cooling has caused the peat accumulation processes to slow down. It has also caused the denudation-depositional processes to become more active. On the whole, the burial of peat on the island during the Late Glacial period and the Holocene was associated with aeolian processes, as well as with lake shore erosion. The lake shore erosion was in turn associated with abrasion caused by water waves and temperatures. During mid-Holocene, erosional processes that transpired along the sea coast started playing their part in the overall picture. Additionally, marine transgressions affected the island deposits at heights that reached 7–10 m asl.

One date deserves particular attention. It is the date of 1285–1335 cal BP ($IGAN_{AMS}5329$/UG_{AMS} 27737) obtained from sample 24-1 (Figure 3), associated with aeolian sands that were transported from the sea coast. Considering the rate of coastline retreat caused by marine abrasion (about 2 m per year), this date points to the old age of the onset of the sand deposition processes. This sample also illustrates the far distance (about 2500 m), over which the sands were transported from the coast.

CONCLUSIONS

There are three stratigraphic levels on Belyi Island. The lowest one corresponds to the Kargin warming (MIS 3) and contains peat, as well as lagoonal deposits that contain detritus and other organic material suitable for ^{14}C dating. The middle level that dates to LGM (MIS 2) contains sands in which no organic materials have been recovered so far. And finally, the upper layer that dates to Holocene and the Late Glacial contains lots of organic material. Dates have been obtained only for the lower and upper stratigraphic levels (MIS 3 and MIS 1). The natures of these deposits vary. In particular, Kargin deposits, which are situated at the base of the stratigraphic column, are usually associated lagoonal deposits that contain detritus.

Deposits associated with the upper level (MIS 1) are more diverse; there are a few types of Holocene and Late Glacial period (MIS 1) deposits that are suitable for ^{14}C dating. They include the following: (1) The very common redeposited sand deposits with organic inclusions and paleo-peat horizons (13,000–1500 cal BP). (2) In situ paleo-peat soils and pedosediments that date to the Early Holocene. For example, the pedosediment that came from the western shore of the island and dated to 10,000–9600 cal BP. (3) In situ peat soils that are not buried. These soils, which are eroded at the top, are quite old (up to 12.7 ka cal BP). (4) Modern aeolian-cumulative peat-sandy soils in the coastal zone, the age of which does not exceed 1500 cal BP. ln addition, there are ancient Kargin layers that formed in the sea coastal zone around 31–40 ka cal BP.

https://doi.org/10.1017/RDC.2018.115 Published online by Cambridge University Press

The dates obtained from Belyi lsland span across the MIS l and MIS 3 periods, which correspond to the Holocene and the Kargin warming stages. This is not surprising because the climate conditions during these periods favored the development and burial of materials, such as peat and organic detritus in the sea clay sediments. The dates from the MIS 2 period are missing. This is due to the conditions of this period being extremely unfavorable for the accumulation of peat, as well as of other materials fit for ^{14}C dating. The relative paucity of dates associated with MIS 3 does not have to reflect harsh climatic conditions. MIS 3 layers are deposited at significant depths, in permafrost conditions, which makes them difficult to examine, especially in the central part of the island. The MIS 2 period was characterized by a deep regression of the world's ocean, associated with the expansion of glaciers. During the MIS 3 period, on the other hand, global sea level was close to its modern mark. This climatic sequence is confirmed by our dates of lagoon sediments, as well as of other marine sediments that are located above the modern sea level. During the MIS 1 period, we can distinguish two main stages. (1) Thermal maximum (ca. 13–9 cal BP), which, besides the Boreal and Preboreal should include the end of the Allerød and the Younger Dryas. (2) A climate cooling period (ca. 9–0 cal BP), which includes the Atlantic, the Subboral, and the Subatlantic. The cooling associated with the Younger Dryas period was significantly weaker than the mid-Holocene one. The accumulation of peat during the Younger Dryas went uninterrupted, with the same intensity as in the Early Holocene.

ACKNOWLEDGMENTS

The ^{14}C dating of soils and sediments by the liquid scintillation counting was supported by the Russian Foundation for Basic Research (project №16-45-890312) and the accelerator mass spectrometry was supported by the Russian Scientific Foundation (grant №14-27-00133). The studies of the evolution of the natural environment were funded by RFBR and Russian Geographical Society according to the research project №17-05-41157. The soils research was supported by the Ministry of Education and Science of the Russian Federation (Agreement №02.A03.21.0008). We also want to express our gratitude to Alexei Titovsky and Vladimir Pushkarev for their help in organizing the expedition and to Artem Yakimov for his participation and help in the field.

REFERENCES

Abakumov EV, Shamilishviliy GA, Yurtaev AA. 2017. Soil polychemical contamination on Beliy Island as key background and reference plot for Yamal region. *Polish Polar Research* 38(3):313–2.

Alexandrovskiy A, Yurtaev A, Skripkin V, Dolgikh A, Yakimov A. 2017. Radiocarbon age of the buried and modern peat soils on the Belyi Island (Kara Sea). *Cryosols in Perspective: A View from the Permafrost Heartland*. August 21–28, Yakutsk, Sakha (Yakutiya) Republic, Russia. p 9–10.

Artemyeva ZS, Yurtaev AA, Alexandrovskiy AL, Zazovskaya EP. 2016. The organic matter of the buried peat soils on Bely Island (Kara Sea). *Byulleten' pochvennogo instituta im. V.V. Dokuchayeva* 85:36–55. In Russian.

Baranskaya AV, Romanenko FA. 2017. Quaternary deposits and paleogeography of the Belyi Island in the Late Pleistocene and Holocene. *Voprosy geomorfologii i paleogeografii morskikh poberezhiy i shel'fa. Materialy nauchnoy konferentsii pamyati Pavla Alekseyevicha Kaplina. Geograficheskiy fakul'tet MGU*:29–32. In Russian.

Baranskaya AV, Romanenko FA, Arslanov HA, Maksimov FE, Starikova AA, Pushina ZV. 2018. Perennially frozen deposits of Bely Island: stratigraphy, age, depositional environments. *Kriosfera Zemli* XXII(2):3–15. In Russian.

Bolshiyanov D, Makarov A, Savelieva L. 2015. Lena River delta formation during the Holocene. *Biogeoscience* 12:579–93.

Bronk Ramsey C. 2013. *OxCal Program v4.2.4*. Oxford: Radiocarbon Accelerator Unit, University of Oxford.

Cheng P, Zhou W, Wang H, Lu X, Du H. 2013. ^{14}C Dating of soil organic carbon (SOC) in loess-paleosol using sequential pyrolysis and accelerator mass spectrometry (AMS). *Radiocarbon* 55(2–3):563–70.

Cherkinsky A, Culp R, Dvoracek D, Noakes J. 2010. Status of the AMS facility at the University of

Georgia. *Nuclear Instruments and Methods in Physics Research B* 268:867–70.

Evseev AV, Svitoch AA. 1979. Buried soils and geochemical features of the newest deposits of the island of Aion (Chaun Bay). *Pochvovedeniye* 11:17–24. In Russian.

FAO-UNESCO Soil Map of the World, Revised Legend, with corrections and updates. 1997. Technical Paper 20. ISRIC. Wageningen.

Gavrilov AV, Romanovskii NN, Hubberten H-W. 2006. Paleogeographic scenario of the postglacial transgression on the Laptev Sea shelf. *Kriosfera Zemli* X(4):39–50. In Russian.

Gubin SV. 1996. Late Pleistocene Soil Formation in Northeast Eurasia. *Doklady AN SSSR* 351 (4):544–47. In Russian.

Kaplin PA. 1975. The recent history of the coasts of the World Ocean. *M.:Izd of MGU*. 265 p. In Russian.

Kaplin PA, Selivanov AO. 1999. Change in the sea level of Russia and the development of the coast. *M.:GEOS*. 316 p. In Russian.

Kaufman DS, Ager TA, Anderson NJ, Anderson PM, Andrews JT, Bartlein PJ, Brubaker LB, Coats LL, Cwynar LC, Duvall ML, Dyke AS, Edwards ME, Eisner WR, Gajewski K, Geirsdóttir A, Hu FS, Jennings AE, Kaplan MR, Kerwin MW, Lozhkin AV, MacDonald GM, Miller GH, Mock CJ, Oswald WW, Otto-Bliesner BL, Porinchu DF, Rühland K, Smol JP, Steig EJ, Wolfe BB. 2004. Holocene thermal maximum in the western Arctic (0–180°W). *Quaternary Science Reviews* 23(5–6):529–60.

Khotinskiy NA. 1977. Holocene of Northern Eurasia: experience of transcontinental correlation of the stages of vegetation and climate development. Nauka. 200 p. In Russian.

Kienast F, Schirrmeister TL, Siegert C, Tarasov P. 2005. Palaeobotanical evidence for warm summers in the East Siberian Arctic during the last cold stage. *Quaternary Research* 63:283–300.

MacDonald GM, Velichko A, Kremenetski C, Borisova O, Goleva A, Andreev A, Cwynar LC, Riding R, Forman S, Edwards T, Aravena R, Hammarlund D, Szeicz J, Gattaulin V. 2000. Holocene Treeline History and Climate Change Across Northern Eurasia. *Quaternary Research* 53:302–1.

Moskovchenko DV, Kurchatova AN, Fefilov NN, Yurtaev AA. 2017. Concentrations of trace elements and iron in the Arctic soils of Belyi Island (the Kara Sea, Russia): patterns of variation across landscapes. *Environ Monit Assess* 189:210.

Reimer PJ, Bard E, Bayliss A, Beck JW, Blackwell PG, Bronk Ramsey C, Grootes PM, Guilderson TP, Haflidason H, Hajdas I, Hatt C, Heaton TJ, Hoffmann DL, Hogg AG, Hughen KA, Kaiser KF, Kromer B, Manning SW, Niu M, Reimer RW, Richards DA, Scott EM, Southon JR, Staff RA, Turney CSM, van der Plicht J. 2013. IntCal13 and Marine13 Radiocarbon Age Calibration Curves 0-50,000 Years cal BP. *Radiocarbon* 55(4):1869–87.

Skripkin VV, Kovalyukh NN. 1998. Recent development in the procedures used at the SSCER Laboratory for the routine preparation of lithium carbide. *Radiocarbon* 40:211–14.

Slagoda EA, Leibman MO, Khomutov AV, Orekhov PT. 2013. Cryolithologic construction of the firstnterrace at Bely Island, Kara Sea (Part 1). *Kriosfera Zemli XVII* (4):11–21. In Russian.

Stein R, Dittmers KH, Fahl K, Kraus M, Matthiessen J, Niessen F, Pirrung M, Polyakova YeI, Schoster F, Steinke T, Fütterer DK. 2004. Arctic (palaeo) river discharge and environmental change:evidence from the Holocene Kara Sea sedimentary record. *Quaternary Science Reviews* 23(11–13):1485–511.

Streletskaya ID, Vasiliev AA, Oblogov GE, Tokarev IV. 2015. Reconstruction of paleoclimate of Russian arctic in Late Pleistocene-Holocene on the basis of isotope study of ice wedges. *Earth's Cryosphere* 19(2):98–106.

Tarasov PE, Andreev AA, Romanenko FA, Sulerzhitskii LD. 1995. Palynostratigraphy of upper Quaternary deposits of Sverdrup Island, the Kara Sea. *Stratigraphy and Geological Correlation* 3:190–96. In Russian.

Vasil'chuk AC. 2017a. Palynological spectra and chronology of poligonalno-zhilnye complexes of Yamal. *Arktica and Antarktika* 1:84–109. In Russian.

Vasil'chuk AC. 2017b. Palynological spectra of Holocene poligonalno-zhilnye structures of the Belyi Island and the valley of the Tabmei River of the Yamal Peninsula. *Arktica and Antarktika* 2:1–24. In Russian.

Vasilchuk YUK, Petrova EA, Serova AK.1983. Some features of the paleogeography of the Holocene of Yamal. *Byulleten' po izucheniyu chetvertichnogo perioda* 52:73–89. In Russian.

Velichko AA, Faustova MA, Pisareva VV, Karpukhina NV. 2017. History of the Scandinavian ice sheet and surrounding landscapes during Valday ice age and the Holocene. *Ice and Snow* 57(3):391–416. In Russian.

Velichko AA, Timireva S N, Kremenetski KV, MacDonald G, Smith L. 2011. West Siberian Plain as a late glacial desert. *Quaternary International* 237:45–53.

Wacker L, Němec M, Bourquin J. 2010. A revolutionary graphitisation system:fully automated, compact and simple. *Nuclear Instruments and Methods in Physics Research B* 268(7–8):931–4.

Zazovskaya E, Mergelov N, Shishkov V, Dolgikh A, Miamin V, Cherkinsky A, Goryachkin S. 2017. Radiocarbon age of soils in oases of East Antarctica. *Radiocarbon* 59(2):489–503.